

# Effect Y substitution on the microstructure, transport and magnetic proprieties of $\text{Bi}_2\text{Sr}_2\text{Ca}_1\text{Cu}_2\text{O}_{8+\delta}$ superconducting ceramics

S. MENASSEL<sup>1,\*</sup>, M.-F. MOSBAH<sup>1,2</sup>, Y. BOUDJADJA<sup>3</sup>, S.P. ALTINTAS<sup>4</sup>, A. VARILCI<sup>4</sup>,  
C. TERZIOGLU<sup>4</sup>

<sup>1</sup>Materials Science and Applications Research Unit, Physics Department, Constantine 1 University,  
B.P. 325 Route d'Ain El Bey, 25017 Constantine, Algeria

<sup>2</sup>National Polytechnic School of Constantine, Ville Universitaire, Nouvelle Ville Ali Mendjeli, Algeria

<sup>3</sup>LEND, Faculty of Science and Technology, Jijel University, BP 98 Ouled Aissa, 18000 Jijel, Algeria

<sup>4</sup>Abant Izzet Baysal University, Department of Physics, 14280 Bolu, Turkey

In high  $T_c$  superconductors (HTSC) the activation energy gives information about the pinning properties of a sample under applied magnetic field. Pinning of vortices determines the critical current density  $J_c$  which is of great importance for practical applications of HTSC. Instead of magnetic measurements, the activation energy may be calculated from resistivity measurements realized under magnetic field. This kind of measurement has been made in this work for yttrium doped samples of  $\text{Bi}_2\text{Sr}_2\text{CaCu}_2\text{O}_{8+\delta}$  (Bi-2212) for different values of applied magnetic field. Samples of  $\text{Bi}_2\text{Sr}_2\text{Ca}_{1-x}\text{Y}_x\text{Cu}_2\text{O}_{8+\delta}$  ( $x = 0, 0.025, 0.1, 0.25$ ) were prepared by a sol-gel method and characterized by X-ray diffraction (XRD), scanning electron microscopy (SEM) and energy dispersive analysis of X-ray. The measurements of resistivity were made using a classical four probe method and DC current. The magnetic field was applied with a constant amplitude of 0 T, 1 T, 2 T and 3 T. The obtained results show that the activation energy decreases with introduction of yttrium, but has a relative maximum when  $x$  is equal 0.1. The decrease of the activation energy is explained by the granular nature of the samples which promotes 3D transition to 2D of the vortex lattice.

Keywords: *high  $T_c$  superconductors; Y substitution; sol-gel method, activation energy, 3D to 2D transition*

© Wrocław University of Technology.

## 1. Introduction

In high  $T_c$  superconducting (HTSC) materials the main parameter for practical applications is, beside the critical temperature of transition  $T_c$ , the critical current density. This parameter, which limits the transport of current carried by the material, is controlled by the capability of pinning vortices under applied magnetic field. This is why activation energy, or pinning potential, was studied earlier in Bi based high  $T_c$  superconducting materials (HTSC) in both single crystals [1–3] and polycrystalline [4, 5] samples. The pinning force balances the Lorentz force. Moving of vortices causes

thermal dissipation which may destroy superconductivity. Near  $T_c$ , the resistive transition corresponds to the “flux flow” dissipative regime [6, 7] where the Lorentz force dominates [1]. Thermal dissipation is possible also when the pinning force dominates and is caused by “flux creep” [8] which is more evident in magnetic measurements [4, 5]. On the other hand, doping by cation has been intensively studied in order to understand the mechanism of high  $T_c$  superconductivity and to improve the properties of the material. Among various atomic elements, the rare earth ones have been used for their capability, when substituting at the Ca site, to reduce the carrier concentration in the  $\text{CuO}_2$  planes of the Bi-2212 phase [9–39]. The case of doping by yttrium has been a subject

\*E-mail: sihem\_menassel@yahoo.fr

of several studies [10–23, 26, 33, 37, 39]. The pinning properties, expressed in the irreversibility line, have been at this time studied in Y substituted Bi-2212 crystals [33]. To our knowledge, no study has been made before about the effect of Y doping on the activation energy of Bi-2212 ceramic samples as it has been made for undoped Bi-2212 crystal [2], and in more recent works on doped and undoped Bi based polycrystalline samples [41–45]. This effect is presented for the case of Y substitution on the Ca site at the rate varying up to 25 % ( $x = 0.25$ ), under applied magnetic field having a constant amplitude equal to 0 T, 1 T, 2 T and 3 T.

## 2. Experimental

Bismuth, strontium, calcium and copper nitrates were dissolved in distilled water in a stoichiometric ratio. Y powder dissolved in nitric acid was added to the Bi solution. A solution of triammonium citrate with a concentration of 2 mol/kg, was prepared by reacting citric acid with ammonia solution. The organic gels were made with acrylamide  $\text{CH}_2=\text{CHCONH}_2$  and N,N-methylene diacrylamide.  $\text{CH}_2=\text{CHCONHCH}_2\text{NHCOCCH}=\text{CH}_2$  was added in order to complex the Bi, Ca, Sr and Cu cations. The obtained solution was mixed, stirred and heated at 80 °C to 90 °C with a magnetic stirrer on a hot plate. Few drops of a solution of AIBN in acetone were added to accelerate the formation of the gel. The later was transformed to Bi-2212 powder after heating at 400 °C for 2 h and 6 h at 700 °C. The obtained powder was ground in an agate mortar and calcined during 12 h at 860 °C with a rate of 5 °C/min. After calcinations, the samples were ground again, and then pelletized under a pressure of 300 MPa. The pellets were then sintered during 12 h at 860 °C with a rate of 5 °C/min.

Samples have been denoted as Y0, Y0025, Y010 and Y025, where the number following Y indicates the values of the rate  $x$  of Y. The formation of the Bi-2212 phase was analyzed by XRD with  $\text{CuK}\alpha$  radiation in the range  $2\theta = 10^\circ$  to  $55^\circ$ . Microstructural and surface morphology of the samples were investigated using scanning electron microscopy (SEM, JEOL 6390-LV). The resistivity

was measured for all samples in the temperature range of 10 K to 125 K using a standard DC four-probe technique with a constant current of 5 mA. The current and voltage contacts were made from a silver paste. The magnetic field was applied parallel to the surface of the pellet and perpendicular to the current flow direction.

## 3. Results and discussion

The XRD patterns of the samples are shown in Fig. 1. The diffraction results show the presence of Bi-2212 phase as a major component. The structure of Bi-2201 was also detected. The lattice parameter  $c$  determined using the software Janna 2006 from the (0 0 1) peaks of the XRD data is given in Table 1. It is observed that the lattice parameter  $c$  decreases significantly with increasing Y content. The  $\text{Y}^{3+}$  cation has a smaller ionic radius than  $\text{Ca}^{2+}$ . This explains the decrease of  $c$  which can be also due to the increase of oxygen content in the system as it has been suggested for Y substitution on Ca site.

Microstructural features were studied using SEM (Fig. 2). The SEM images of all samples were taken at a magnification of 3000. The microstructure of Y0 sample is remarkably different from that of Y0025, Y010, and Y025 samples. One can observe that doping with yttrium decreases the size of the grains and deteriorates the surface morphology.

The resistivities recorded under different applied magnetic fields are reported for all the samples in Fig. 3. These records are normalized to the value  $\rho_n$  of the resistivity at 100 K where the samples are supposed to be in their normal state and near the beginning of the superconducting transition. The curves in Fig. 3 show that the applied magnetic field increases the broadening of the transition whose shape depends on the rate of yttrium. Two temperatures are indicated by arrows in the figure to characterize the broadening: the critical temperature  $T_{c0}$  indicates the end of the zero resistance state and, in the transition, a threshold temperature  $T_t$  where the different curves are no longer separated. The values of these temperatures ( $T_{c0\text{max}}$  and  $T_{c0\text{min}}$ ) have been measured without and with

Table 1. Cell parameters (a, b, c), cell volume V, agreement factors (Rp) and goodness of fit (GOF) for the samples; values of the temperatures of transition onset:  $T_{c,onset}$ ,  $T_{c0max}$  and  $T_{c0min}$  indicate the end of the zero resistance state without and with maximum applied magnetic field, respectively.

	a [Å]	b [Å]	c [Å]	V [Å <sup>3</sup> ]	Rp [%]	GOF	$T_{c,onset}$	$T_{c0min}$	$T_{c0max}$
Y0	5.373657	5.401022	30.80966	894.1925	7.65	1.19	88	36.4	53.7
Y0025	5.373845	5.386960	30.60010	885.8328	10.28	2.94	82.4	11.8	27.8
Y010	5.391014	5.386136	30.51944	886.1846	10.15	3.46	106	28.7	37.8
Y025	5.401697	5.389121	30.30481	882.1852	8.83	2.47	90.5	6	13.6

applied magnetic field) together with the critical transition onset temperature  $T_{c,onset}$ .

These results show that doping with Y increases the width of the transition and lowers the  $T_{c0}$ . Applying magnetic field increases the width of the transition in the doped samples more than in the undoped ones. The enhancement in the undoped sample for 3 Tesla is about 7.3 K and goes from 16 K to 7.6 K as the content of Y increases. This enhancement is roughly equal to the decrease of  $T_{c0}$  except for the undoped sample where the decrease of  $T_{c0}$  is higher. Moreover, the variation of  $T_{c0}$  with magnetic field is higher in the undoped samples than in the doped ones. The shape of the transition varies also from the undoped samples to the doped ones and with the content of Y. In the doped samples, the transition presents a kind of knee much more evident in samples Y0025 and Y025 at about 30 K. The knee is also present for 0 T at about 50 K for Y0025 and 45 K for Y025. In samples Y0 and Y010, the knee is not present at 0 T, but appears with magnetic field at about 60 K in Y010.

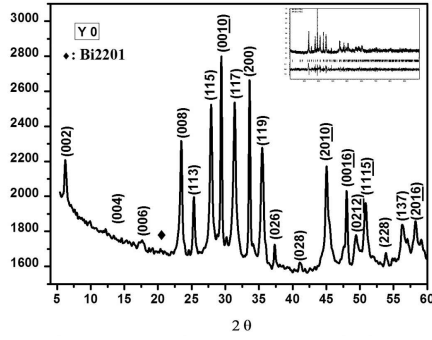
In sample Y025, under magnetic field, the resistivity varies slowly between  $T_t$  and 30 K (position of the knee). This kind of shape (the knee) has been seen in measurements of resistivity of Bi-2212 crystals with magnetic field applied perpendicular to ab planes when the configuration of the applied current and field has not resulted in any Lorentz force [46–48]. In the last case, the resistivity shows an important enhancement before the sharp decrease of the superconducting transition. Such behavior, as shown by several authors [47–52], indicates a transition from a gas of 2D pancake vortices to a liquid of 3D vortices, and is above the irreversibility line in the (H,T) plane.

In the ceramic samples studied here, the grains have plate-like shape where the largest dimension is along ab planes. When a magnetic field is applied perpendicular to these plates, their individual demagnetizing field coefficient  $N_g$  along the same direction increases the field by a factor  $1/(1 - N_g)$  ( $N_g \leq 1$ ) [53]. Curves in Fig. 3 suggest that in samples Y0025 and Y025 more grains have their ab planes oriented perpendicular to the applied field. Moreover,  $N_g$  gives a much higher effective field which destroys the conduction of the Josephson junctions, forming the weak links between the grains, but this behavior is supposed to occur at low field.

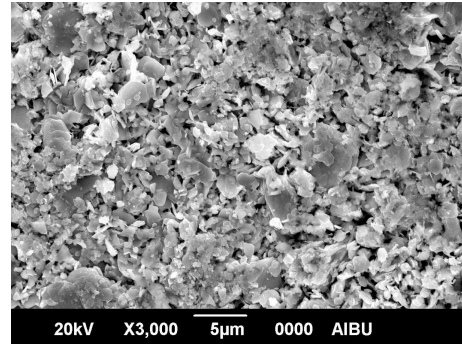
Fig. 4 shows the Arrhenius plot of the natural logarithm of the normalized resistivity of the samples ( $\ln(\rho/\rho_{100})$  versus  $1/T$ ). This figure gives a better view of how the yttrium doping changes the effect of magnetic field at low temperatures. The horizontal scale is the same in Fig. 4a and Fig. 4c but different in Fig. 4b and Fig. 4d, where there is a multiplication of about five. Without yttrium (sample Y0 in Fig. 4a) the curves are well separated and the absolute value of their slope at low temperatures decreases with the strength of the magnetic field. With yttrium, the magnetic field moves the curves toward much lower temperatures (higher values of  $1/T$ ) but their separation is smaller and they are almost identical as for sample Y0025 (Fig. 4b).

These curves allow the calculation of the activation energy as suggested by the model of “flux creep” [7]. In this case, the resistivity obeys the law:

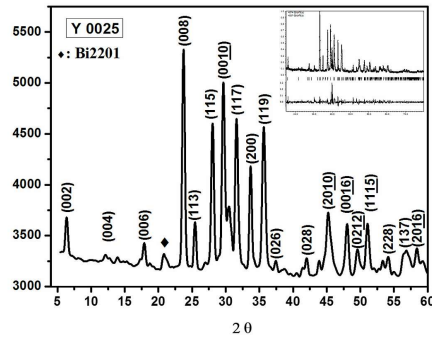
$$\rho(H, T) = \rho_0 \exp(-U_0(H)/k_B T) \quad (1)$$



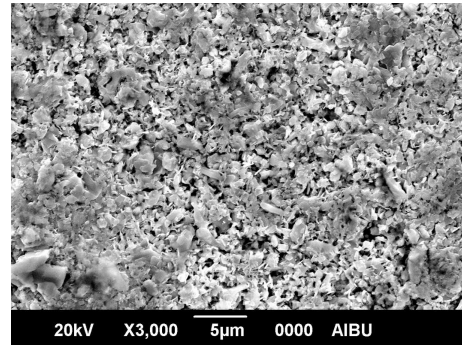
(a)



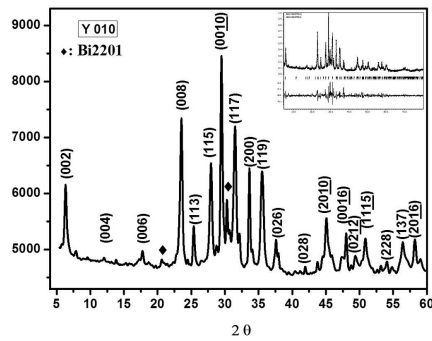
(a)



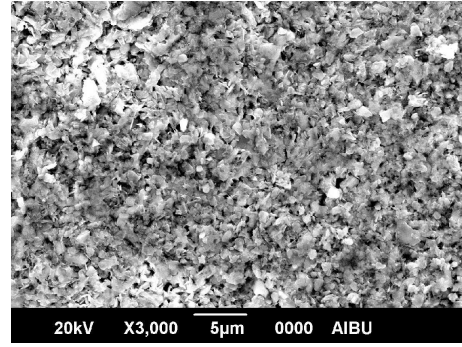
(b)



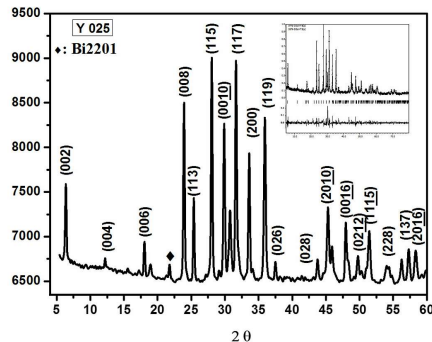
(b)



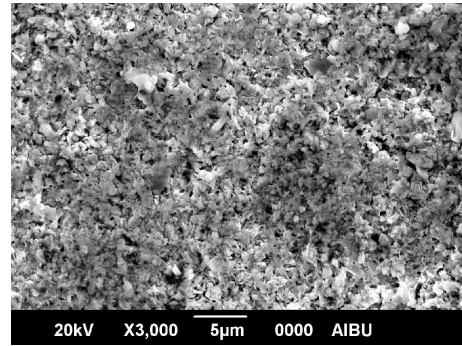
(c)



(c)



(d)



(d)

Fig. 1. The XRD patterns for Y0, Y0025, Y010 and Y025 samples.

Fig. 2. SEM images of the samples Y0, Y0025, Y010 and Y025.

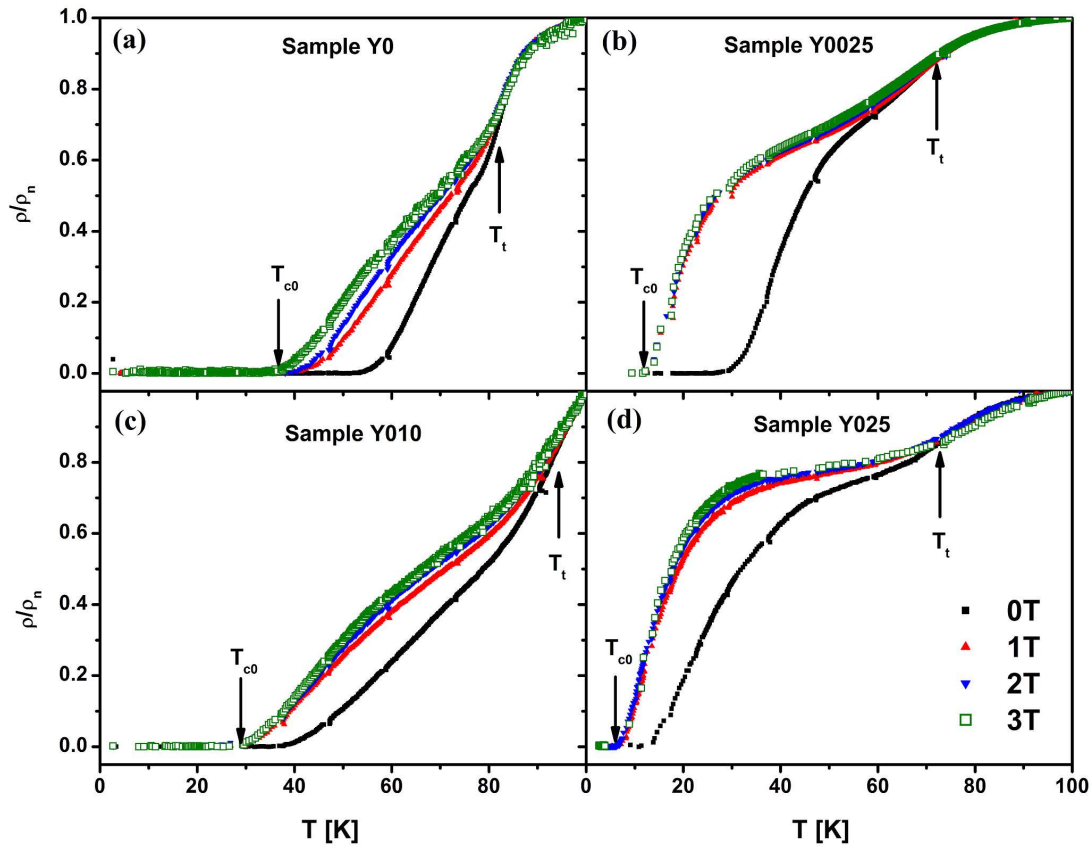


Fig. 3. Resistivity  $\rho(T)$  normalized against the value  $\rho_n$  at 100 K for (a) sample Y0, (b) sample Y0025, (c) sample Y010 and (d) sample Y025. The arrows in each figure indicate  $T_{c0}$  where the zero resistance state ends (here for maximum applied field) and the threshold temperature  $T_t$  in the transition where the curves are no longer separated.

where  $U_0$  is the activation energy,  $k_B$  the Boltzmann constant and  $\rho_0$  is a pre-factor to be determined. The slope of  $\ln(\rho/\rho_0)$  in the Arrhenius plot gives the value of  $U_0/k_B$ .

The problem is to limit the range of temperature where this slope may be calculated by a fit to a linear regression using the least square method. The values of  $\rho/\rho_0$  used by other authors [2] were much lower than 0.1 reaching about  $10^{-6}$ . The value of 0.1 has currently been used to estimate the irreversibility field  $H_{irr}$ . For the estimation of  $U_0$ , the curves were taken for values of  $\rho/\rho_0$  between 0.1 and a value corresponding to the deviation from linearity. The obtained values verify the criterion of  $U_0 > k_B T$  which limits the “flux creep” regime and where the “flux flow” regime begins.

The variation of  $U_0$  versus the applied magnetic field  $H$  is revealed for each sample in Fig. 5. This figure shows that  $U_0$  decreases when yttrium is introduced. For  $H \neq 0$ , this decrease goes through a maximum with the rate  $x$  of doping. There is also a decrease of  $U_0$  with  $H$  except for sample Y010 where it remains quasi constant.

The obtained values of  $U_0$  lie between 0.003 eV and 0.060 eV corresponding to about 30 to 750 K. These values are the same as those obtained in Bi-2212 crystal by Shi *et al.* [2]. The last authors used a modified law based on a field dependent activation energy  $U_0 = A(H)(1-T/T_c)^m$  suggested by Yeshurun *et al.* [54]. Shi *et al.* [2] explained in this way the curvature of the Arrhenius plot in their results. This curvature, which occurs in most

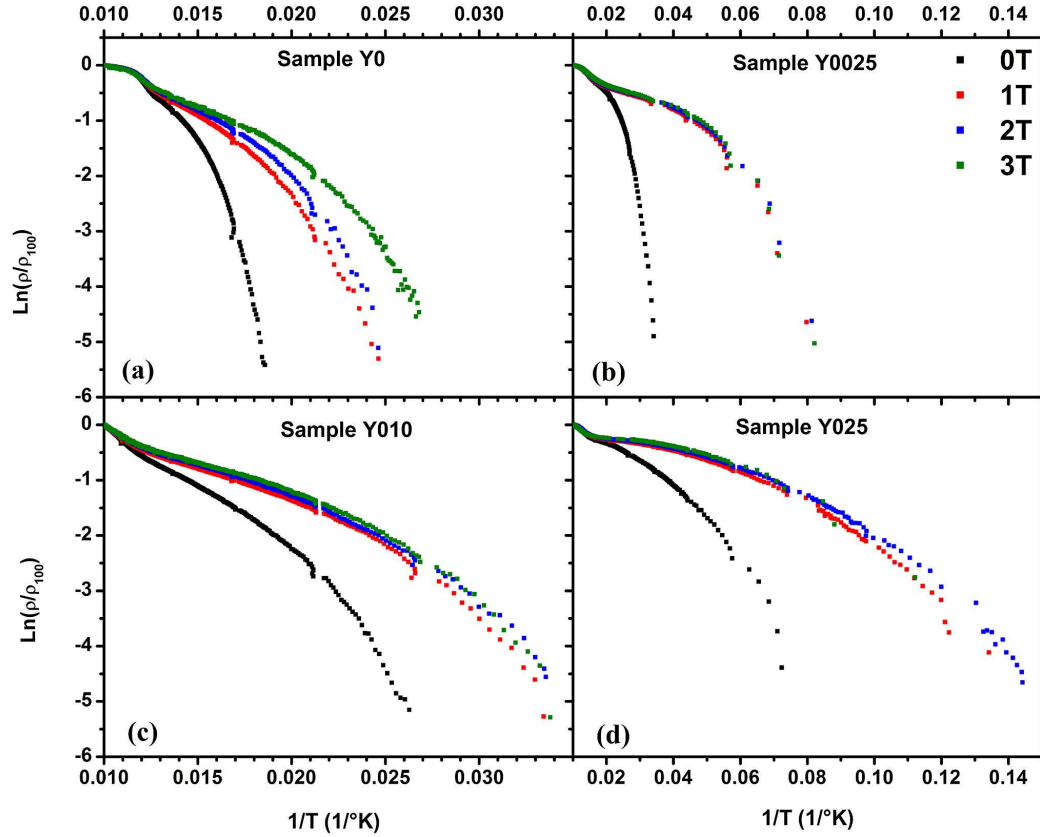


Fig. 4. Arrhenius plots of the natural logarithm of reduced resistivity for samples (a) Y0, (b) Y0025, (c) Y010 and (d) Y025.

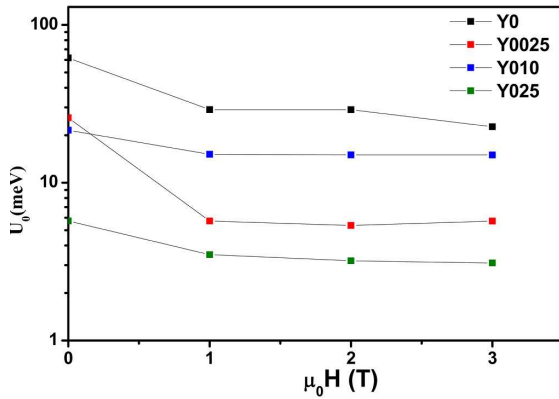


Fig. 5. The dependence of the activation energy  $U_0$  versus magnetic field.

of the cited works, is evident in the results presented in Fig. 4. Nearly the same values of  $U_0$  were also obtained by Sharma et al. [45] in the measurements up to 14 T on Bi-2212 polycrystalline

samples, prepared by sol-gel method and annealed between 760 °C and 840 °C, where they showed an influence of annealing temperature on  $U_0$ . With lead containing (Bi,Pb)2212 samples doped by a rare earth on Sr site the obtained values are much higher, 0.075 eV to 0.308 eV with an applied field of 0.28 T for Gd doping [40] and 0.077 eV to 0.47 eV with an applied field of 0.32 T and 0.63 T for Tb doping [41].

The effect of yttrium is also evident in the plot of the natural logarithm of normalized resistivity ( $\ln(\rho/\rho_{100})$ ) versus the normalized temperature ( $U_0/T$ ) shown in Fig. 6. These curves have been plotted for the same values of  $\rho/\rho_{100}$  as those used for the estimation of  $U_0$ .

Fig. 6 shows that for  $H \neq 0$ , the different curves become less separated as the content of yttrium increases. In the undoped sample Y0 (Fig. 6a), the curves are well separated. Moreover, the curve

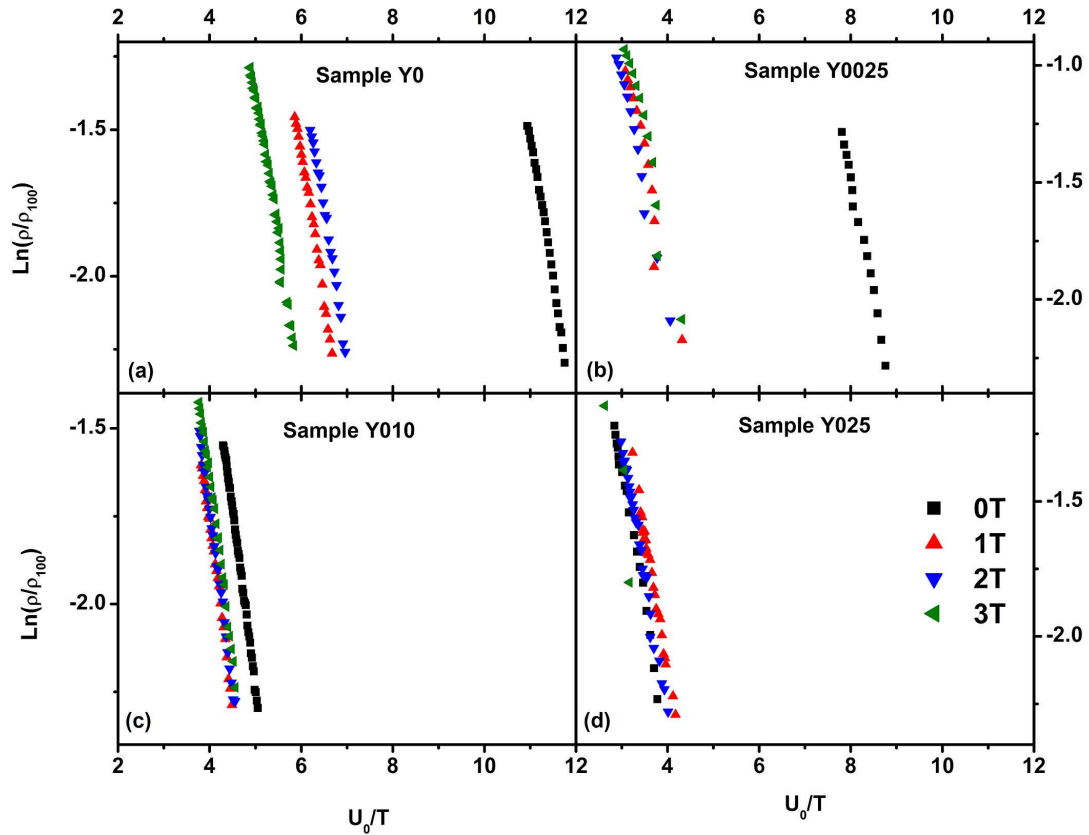


Fig. 6. Dependence of the natural logarithm of normalized resistivity ( $\ln(\rho/\rho_{100})$ ) of the samples on normalized temperature ( $U_0/T$ ).

obtained without applied magnetic field ( $H = 0$ ) is obviously separated from the curves with applied field in samples Y0 and Y0025.

The results shown in Fig. 7 give information on the pre-factor corresponding to the intercept of curves in the limit  $1/T \rightarrow 0$ . This intercept has been calculated for the curves shown in Fig. 6 for the Y doped Bi-2212 samples. The behavior observed in Fig. 6 is confirmed by the intercept, which has a quasi-constant value when  $H \neq 0$  in the samples doped with Y (Y0025, Y010 and Y025). Moreover, the intercept is very different when  $H = 0$  in the samples Y0 and Y0025, which confirms the behavior observed in Fig. 6a and Fig. 6b.

Karppinen *et al.* [55] showed that doping with yttrium at Ca site gives, for the concentrations used in our samples (remark:  $x$  corresponds to  $1 - x$  in that work), an overdoped Bi-2212 phase which is nearly optimally doped for Y010 and Y025.

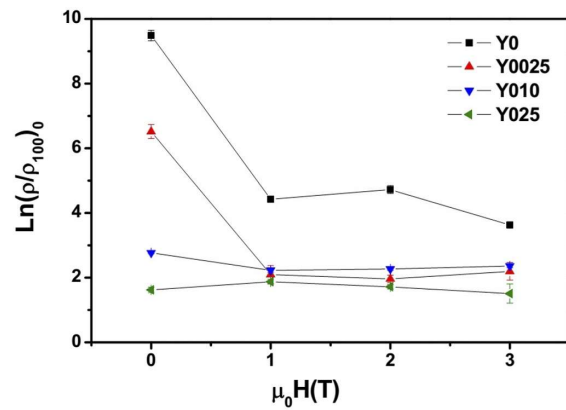


Fig. 7. Intercept of the curves from Fig. 6 in the limit  $1/T \rightarrow 0$ .

Increasing  $x$  decreases the  $c$  axis parameter of the unit cell but the number of holes increases in both  $\text{CuO}_2$  plane and  $\text{BiO}$  layer [55]. The variation of the  $c$  axis parameter changes the coupling

between the coupling of  $\text{CuO}_2$  planes by changing their distance and thus their Josephson coupling. The electromagnetic coupling of the pancake vortices is also influenced by these variations. The variation of the density of holes influences the  $T_c$ . Thus, 3D to 2D transition of the vortices is influenced by these variations. When the  $c$  axis parameter changes, the transition field, where the 3D vortices lattice becomes a 2D vortices gas, changes also. A similar effect is obtained when  $T_c$  changes, but for the temperature of the 3D to 2D transition.

On the other hand, the texture and the granular quality of the sample may influence also the 3D to 2D transition. The angle between  $H$  and the  $ab$  planes is not constant in granular samples and its distribution is more random when the texture is not good. There is also a distribution of the shape and size of the grains and consequently of their demagnetizing factor  $N_g$ . These characteristics combined with a possible lack of homogeneity in yttrium distribution may give grains, in which the vortices form a 3D liquid lattice and other a 2D vortices gas. Fig. 3b and Fig. 3d suggest a higher number of grains with 2D vortices gas in samples Y0025 and Y025 than in the other samples. This may explain the lower activation energy found in these samples (Fig. 5). Fig. 6 shows that when there is yttrium and the field is applied, the curves overlap. Increasing the concentration of yttrium the overlap is more and more obvious. This effect is a consequence of several changes induced by doping with yttrium, such as density of holes in  $\text{CuO}_2$  planes, length of  $c$  axis parameter and texture of the ceramic sample. More investigations on how these changes can influence the 3D to 2D transition of the vortex lattice are needed.

## 4. Conclusion

Yttrium lowers the activation energy of the Bi-2212 phase when it substitutes at the Ca site, for concentrations less or equal to 25 %, at the applied field up to 3 T. The shape of various resistive transitions indicates that this effect is mostly a consequence of the granular nature of prepared samples rather than the variations of the density of

holes in the  $\text{CuO}_2$  planes or the  $c$  axis parameter. When the texture is poor, an important part of the grains may be oriented in the magnetic field so as to promote a 3D to 2D transition of the vortex lattice. The effect is more evident in the higher part (higher values of temperature near  $T_{c,\text{onset}}$ ) of the superconductive transition than in its lower part (lower values of temperature near  $T_{c0}$ ) where the resistivity decrease obeys the usual exponential law corresponding to a flux creep of the vortex lattice.

## Acknowledgements

This work was made under support of the CNEPRUD00920110014 Algerian Government Project in the Abant Izzet Baysal University of Bolu in Turkey.

## References

- [1] PALSTRA T.T.M., BATLOGG B., SCHNEEMEYER L.F., WASZCZAK J.V., *Phys. Rev. Lett.*, 61 (1988), 1662.
- [2] SHI D., KOUROUS H.E., XU M., KIM D.H., *Phys. Rev. B*, 43 (1991), 514.
- [3] NAGANO Y., FUJII T., SHIRAFUJI J., *Jpn. J. Appl. Phys. Lett.*, 30 (1991), L568.
- [4] KUMAKURA H., TOGANO K., YANAGISAWA E., TAKAHASHI K., NAKAO M., MAEDA H., *Jpn. J. Appl. Phys. Lett.*, 28 (1989), L24.
- [5] ROSE R.A., OTA S.B., GROOT DE P.A., JAYARAM B., *Physica C*, 170 (1990), 51.
- [6] HEMPSTEAD C.F., KIM Y.B., *Phys. Rev. Lett.*, 12 (1964), 145.
- [7] TINKHAM M., *Phys. Rev. Lett.*, 13 (1964), 804.
- [8] ANDERSON P.W., *Phys. Rev. Lett.*, 9 (1962), 309.
- [9] BOUDJADJA Y., AMIRA A., SAOUDEL A., VARILCI A., ALTINTAS S.P., TERZIOGLU C., *Physica B*, 443 (2014), 130.
- [10] YOSHIZAKI R., SAITO Y., ABE Y., IKEDA H., *Physica C*, 152 (1988), 408.
- [11] TARASCON J.M., BARBOUX P., HULL G.W., RAMESH R., GREENE L.H., GIROUD M., HEGDE M.S., MCKINNON W.R., *Phys. Rev. B*, 39 (1989), 4316.
- [12] OASHI T., KUMAGAI K., NAKAJIMA Y., TOMITA T., FUJITA T., *Physica C*, 157 (1989), 315.
- [13] GANGULI A.K., NAGARAJAN R., NANJUNDASWAMY K.S., RAO C.N.R., *Mater. Res. Bull.*, 24 (1989), 103.
- [14] MAEDA A., HASE M., TSUKADA I., NODA K., TAKEBAYASHI S., UCHINOKURA K., *Phys. Rev. B*, 41 (1990), 6418.
- [15] MITZI D.B., LOMBARDO L.W., KAPITULNIK A., LADDERMAN S.S., JACOWITZ R.D., *Phys. Rev. B*, 41 (1990), 6564.
- [16] ONOZUKA T., IWABUCHI Y., FUKASE T., SATO H., MITCHELL T.E., *Phys. Rev. B*, 43 (1991), 13066.
- [17] MANDAL P., PODDAR A., GHOSH B., CHOUDHURY P., *Phys. Rev. B*, 43 (1991), 13102.

- [18] MANDRUS D., FORRO L., KENDZIORA C., MIHALY L., *Phys. Rev. B*, 44 (1991), 2418.
- [19] MAZAKI H., KAKIHANA M., YASUOKA H., *Jpn. J. Appl. Phys.*, 30 (1991), 38.
- [20] MANDRUS D., FORRO L., KENDZIORA C., MIHALY L., *Phys. Rev. B*, 45 (1992), 12640.
- [21] KENDZIORA C., FORRO L., MANDRUS D., HARTGE J., STEPHENS P., MIHALY L., REEDER R., MOECHER D., RIVERS M., SUTTON S., *Phys. Rev. B*, 45 (1992), 13025.
- [22] QUITMANN C., ANDRICH D., JARCHOW C., FLEUSTER M., BESCHOTEN B., GÜNTHERODT G., MOSHCHALOV V.V., MANTE G., MANZKE R., *Phys. Rev. B*, 46 (1992), 11813.
- [23] MANDAL J.B., KESHRI S., MANDAL P., PODDAR A., DAS A.N., GHOSH B., *Phys. Rev. B*, 46 (1992), 11840.
- [24] AWANA V.P.S., AGARWAL S.K., NARLIKAR A.V., DAS M.P., *Phys. Rev. B*, 48 (1993), 1211.
- [25] PRABHU P.S., RAO M.S.R., VARADARAJU U.V., RAO G.V.S., *Phys. Rev. B*, 50 (1994), 6929.
- [26] MACKENZIE A.P., OREKHOV Y.F., ZAVARITSKY V.N., *Physica C*, 235 – 240 (1994), 529.
- [27] QUITMANN C., BESCHOTEN B., KELLEY R.J., GÜNTHERODT G., ONELLION M., *Phys. Rev. B*, 51 (1995), 11647.
- [28] GASUMYANTS V.E., AGEEV N.V., VLADIMIRSKAYA E.V., SMIRNOV V.I., KAZANSKIY A.V., KAYDANOV V.I., *Phys. Rev. B*, 53 (1996), 905.
- [29] AWANA V.P.S., MENON L., MALIK S.K., *Phys. Rev. B*, 53 (1996), 2245.
- [30] HARRIS J.M., SHEN Z.-X., WHITE P.J., MARSHALL D.S., SCHABEL M.C., ECKSTEIN J.N., BOZOVIC I., *Phys. Rev. B*, 54 (1996), R15665.
- [31] SANADA N., NAKADAIRA T., SHIMOMURA M., SUZUKI Y., FUKUDA Y., NAGOSHI M., SYONO Y., TACHIKI M., *Physica C*, 263 (1996), 286.
- [32] THAMIZHAVEL A., PRABHAKARAN D., JAYAVEL R., SUBRAMANIAN C., *Physica C*, 275 (1997), 279.
- [33] VILLARD G., PELLOQUIN D., MAIGNAN A., WAHL A., *Physica C*, 278 (1997), 11.
- [34] LI X.G., SUN X.F., TOH Y.H., HSU Y.Y., KU H.C., *Phys. Rev. B*, 58 (1998), 1000.
- [35] SUN X., ZHAO X., WU W., FAN X., LI X.G., *Physica C*, 305 (1998), 227.
- [36] SUN X., ZHAO X., WU W., FAN X., LI X.G., KU H.C., *Physica C*, 307 (1998), 67.
- [37] KIMA D.K., CHOY J.H., OSADA M., KAKIHANA M., YOSHIMURA M., *Solid State Ionics*, 108 (1998), 291.
- [38] SUN X.F., ZHAO X., LI X.G., KU H.C., *Phys. Rev. B*, 59 (1999), 8978.
- [39] GAOJIE X., QIRONG P., ZEJUN D., LI Y., YUHENG Z., *Phys. Rev. B*, 62 (2000), 9172.
- [40] ZHAO X., SUN X.F., WANG L., ZHOU Q.F., WU W.B., LI X.G., *Physica C*, 336 (2000), 131.
- [41] VINU S., SARUN P.M., SHABNA R., BIJU A., SYAMAPRASAD U., *Mater. Lett.*, 62 (2008), 4421.
- [42] VINU S., SARUN P.M., SHABNA R., BIJU A., SYAMAPRASAD U., *J. Alloy. Compd.*, 477 (2009), L13.
- [43] ÖZKURT B., ÖZÇELİK B., *J. Low Temp. Phys.*, 156 (2009), 22.
- [44] ERDEM M., ÖZTURK Ö., YUCEL E., ALTINTAS S.P., VARILCI A., TERZIOGLU C., BELENLI I., *Physica B*, 406 (2011), 705.
- [45] SHARMA D., KUMAR R., AWANA V.P.S., *Solid State Commun.*, 152 (2012), 941.
- [46] BRICENO G., CROMMIE M.F., ZETTL A., *Phys. Rev. Lett.*, 66 (1991), 2164.
- [47] HELLERQVIST M.C., RYU S., LOMBARDO L.W., KAPITULNIK A., *Physica C*, 230 (1994), 170.
- [48] CHO J.H., MALEY M.P., FLESHLER S., LACERDA A., BULAEVSKII L.N., *Phys. Rev. B*, 50 (1994), 6493.
- [49] BLASIUS T., NIEDERMAYER C., TALLON J.L., POOKE D.M., GOLNIK A., BERNHARD C., *Phys. Rev. Lett.*, 82 (1999), 4926.
- [50] KUCERA J.T., ORLANDO T.P., VIRSHUP G., ECKSTEIN J.N., *Phys. Rev. B*, 46 (1992), 11004.
- [51] THOPART D., GOUPIL C., SIMON C., *Phys. Rev. B*, 63 (2001), 184504.
- [52] DARMINTO D., MENOVSKY A.A., TJIA M.O., *Phys. Rev. B*, 67 (2003), 012503.
- [53] SENOUSI S., *J. Phys. III France*, 2 (1992), 1041.
- [54] YESHURUN Y., MALOZEMOFF A.P., *Phys. Rev. Lett.*, 60 (1988), 2202.
- [55] KARPPINEN M., KOTIRANTA M., NAKANE T., YAMAUCHI H., CHANG S.C., LIU R.S., CHEN J.M., *Phys. Rev. B*, 67 (2003), 134522.

Received 2015-11-26

Accepted 2016-06-03